# The Significant Influence of a Second Metal on the Antiproliferative Properties of the Complex [Ru($\eta^6$–$C_{10}H_{14}$)($Cl_2$)(dmoPTA)]

Nazanin Kordestani,[a] Elisa Abas,[b] Laura Grasa,[b, c, d] Andres Alguacil,[a] Franco Scalambra,[a] and Antonio Romerosa*[a]

**Abstract:** Complexes [Ru($\eta^6$–$C_{10}H_{14}$)($Cl_2$)(HdmoPTA)]($OSO_2CF_3$) (**1**), [Ru($\eta^6$–$C_{10}H_{14}$)($Cl_2$)(dmoPTA)] (**2**) and [Ru($\eta^6$–$C_{10}H_{14}$)($Cl_2$)-μ-dmoPTA-1κ*P*:2κ$^2$*N*,*N*′-$MCl_2$] (M=Zn (**3**), Co (**4**), Ni (**5**), dmoPTA = 3,7-dimethyl-1,3,7-triaza-5-phosphabicyclo[3.3.1]nonane) have been synthesized and characterized by elemental analysis and spectroscopic techniques. The crystal structures of **1**, **3** and **5** were obtained by single-crystal X-ray diffraction. The antiproliferative activity of the complexes was evaluated against colon cancer cell line Caco-2/TC7 by using the MTT protocol. The monometallic ruthenium complexes **1** and **2** were found to be inactive, but the bimetallic complexes **3**, **4** and **5** display an increased activity ($IC_{50}$ **3**: 9.07 ± 0.27, **4**: 5.40 ± 0.19, **5**: 7.15 ± 0.30 μM) compared to cisplatin ($IC_{50}$ = 45.6 ± 8.08 μM). Importantly, no reduction in normal cell viability was observed in the presence of the complexes. Experiments targeted to obtain information on the possible action mechanism of the complexes, such as cell cycle, ROS and gene expression studies, were performed. The results showed that the complexes display different properties and action mechanism depending on the nature of metal, M, bonded to the $CH_3N_{dmoPTA}$ atoms.

## Introduction

Platinum complexes are the metal compounds most used against cancer, making up more than 50% of current chemotherapeutic treatments. One of the most popular and the first known antiproliferative platinum complexes is *cis*-[$PtCl_2(NH_3)_2$], namely cisplatin.[1] Nevertheless, it is well known that the use of Pt complexes in cancer treatment is also accompanied by serious side effects and drawbacks related to their low selectivity and the development of drug resistance.[2] Among the alternatives investigated to overcome the problems related to Pt-containing drugs, ruthenium complexes have been revealed to be valuable tools,[3] displaying three good properties for medicinal applications: a) an adequate ligand-exchange rate, b) a range of accessible oxidation states (II, III, IV), and c) the facility to mimic iron binding with a wide variety of biological molecules.[4] The extensive and pioneering work by Sadler and co-workers on the antitumor properties of organometallic piano-stool ruthenium compounds showed their effective antiproliferative activity, also shedding light on the mechanism of interaction with some key biomolecules.[5] However, the very low solubility and stability in water of many ruthenium organometallic complexes limit their use as antiproliferative agents. The solubility of ruthenium compounds has been increased by using dialkyl sulfoxide derivatives, such as in [*trans*-$RuCl_4$(DMSO)Im][ImH] (NAMI–A), which entered clinical trials,[6] and by the use of water-soluble phosphines. In 2001, Dyson et al. reported a ruthenium complex containing *p*-cymene and the water-soluble phosphine 1,3,5-triaza-7-phosphaadamantane (PTA), which displayed significant antiproliferative activity against both cisplatin-resistant and nonresistant cancer cells.[7] This was the first example of the known large family of RAPTA complexes, which has been deeply studied due to the interesting antiproliferative profile shown by some of its members.[8] Recent reviews have been targeted to describe the antiproliferative properties of the complexes containing PTA and its derivatives[9] and RAPTA complexes.[10]

Inspired by these findings, we published the water-soluble ruthenium cyclopentadienyl complexes containing hydrosoluble phosphines with the general formula [RuCpX(L)(L′)]$^{n+}$ (X=Cl, I; L=$PPh_3$; L′=PTA, mPTA; L=L′=PTA, mPTA. mPTA = *N*-methyl-1,3,5-triaza-7-phosphaadamantane),[11] which are stable in water

[a] Dr. N. Kordestani, A. Alguacil, Dr. F. Scalambra, Prof. A. Romerosa
Área de Química Inorgánica-CIESOL
Facultad de Ciencias, Universidad de Almería
Carr. Sacramento, s/n, 04120 La Cañada, Almería (Spain)
E-mail: romerosa@ual.es
[b] Dr. E. Abas, Dr. L. Grasa
Departamento de Farmacología, Fisiología y Medicina Legal y Forense
Facultad de Veterinaria, Universidad de Zaragoza
Miguel Servet, 177, 50013, Zaragoza (Spain)
[c] Dr. L. Grasa
Instituto de Investigación Sanitaria de Aragón (IIS Aragón)
San Juan Bosco, 13, 50009, Zaragoza (Spain)
[d] Dr. L. Grasa
Instituto Agroalimentario de Aragón -IA2- (Universidad de Zaragoza–CITA)
Miguel Servet, 177, 50013, Zaragoza (Spain)

Supporting information for this article is available on the WWW under https://doi.org/10.1002/chem.202103048

solution against both hydrolysis and oxidation by oxygen and showed remarkable activity towards DNA depending on the nature of the ligands (water-soluble phosphines and halogen). Further achievements were published by substitution of the halogen by natural purines and thiopurines, which showed to be more active than their respective parent complexes and also than cisplatin against T2 (cisplatin-sensitive) and SKOV3 (cisplatin-resistant) cell lines.[12] When PTA was substituted by derivatives such as the water-soluble phosphines *N*-methyl-1,3,5-triaza-7-phosphaadamantane (mPTA) and $NaPPh_2(3\text{-}SO_3\text{–}C_6H_4)$ (mTPPMS), the antiproliferative activity of the resulting complexes was modulated.[13] As a consequence of these studies, new PTA derivatives were obtained such as *N*,*N*′-dimethyl-1,3,5-triaza-7-phosphaadamantane (dmPTA) and 3,7-H-3,7-dimethyl-1,3,7-triaza-5-phosphabicyclo[3.3.1]nonane (HdmoPTA), which can be easily deprotonated to generate the neutral 3,7-dimethyl-1,3,7-triaza-5-phosphabicyclo[3.3.1]nonane (dmoPTA).[14] This ligand can coordinate to metals by the soft P and the two hard $NCH_3$ atoms, acting by this coordination position as a six-membered chelate.[15] This property led to the synthesis of a variety of different Ru–M bis-heterometallic complexes with the general formula $[RuCp(L)(PPh_3)\text{-}\mu\text{-}dmoPTA\text{-}1\kappa P\text{:}2\kappa^2 N,N'\text{-}ML'_2]$ (M=Co, Ni, Zn; L=Cl, $PPh_3$; L′=Cl, acac-$\kappa^2$O,O′), which showed high antiproliferative activity, significantly higher than cisplatin.[16] Among them, the bismetallic complex $[RuCp(PPh_3)_2\text{-}\mu\text{-}dmoPTA\text{-}1\kappa P\text{:}2\kappa^2 N,N'\text{-}ZnCl_2](CF_3SO_3)$ showed the highest cytotoxicity against a panel of tumor cells (A549 (lung), HBL-100 (breast), T-47D (breast), SW1573 (lung), HeLa (cervix), WiDr (colon)), being 26–426 times more active than cisplatin. This complex also showed good selectivity for cancer cells as it displayed three times lower toxicity against the nontumor human cell line BJ-hTert.[17] These results evidenced that the dimethylation of the PTA ligand and the further coordination of a metallic moiety to the Ru-dmoPTA scaffold are key points for what concern the structure-activity relationship (SAR) of this class of compounds. So far, the questions related to the present work became evident: is it possible to improve the activity of the RAPTA complexes by substitution of the PTA by a dmoPTA ligand? Also, do bismetallic complexes possibly display a higher antiproliferative activity? Is the mechanism of action the same for mononuclear Ru complex and bis-metallic Ru–M complexes? In this paper, we try to answer some of these questions, and others will be tentatively resolved.

## Results and Discussion

The ruthenium complex $[Ru(\eta^6\text{–}C_{10}H_{14})(Cl_2)(dmoPTA\text{-}\kappa P)](OSO_2CF_3)$ (**1**) containing *p*-cymene and dmoPTA was obtained by using stoichiometric amounts of $[Ru(\eta^6\text{–}C_{10}H_{14})Cl_2]_2$ and dmPTA in ethanol at 65 °C for 2 h (Figure 1).

The $^{31}P\{^1H\}$ NMR spectrum of the obtained product shows a unique singlet at −9.30 ppm in MeOD (Figure S4 in the Supporting Information), which is similar to the $^{31}P$ resonance observed for HdmoPTA in complexes $[RuClCp(PPh_3)(HdmoPTA)](CF_3SO_3)$ (−6.34 ppm)[14] and $[RuCp(PPh_3)_2(HdmoPTA)](OSO_2CF_3)$ (−13.94 ppm).[16c] The $^1H$ NMR (Figure S2) shows the presence of one molecule of *p*-cymene and one HdmoPTA coordinated to the metal, arising the corresponding signals in the same range as those for published similar compounds.[8,17] The formation of **1** was also corroborated by $^{13}C\{^1H\}$ NMR (Figure S3). Finally, the elemental analysis fits with the presence of two chlorides, which complete the coordination sphere of the metal and the IR spectrum (Figure S1) revealed that a triflate anion is balancing the charge. The proposed composition of the complex was finally supported by single-crystal X-ray diffraction (Figure 2).

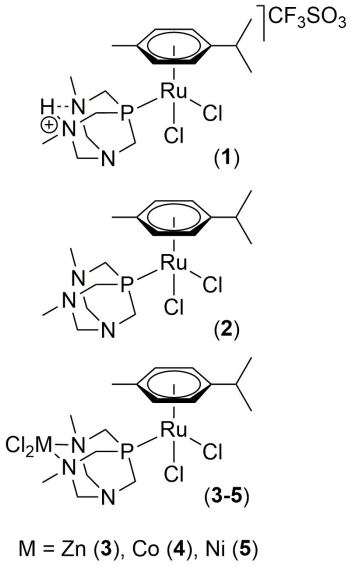


**Figure 1.** Structures of **1**–**5**.

Reacting complex **1** with *t*BuOK in dry methanol affords the deprotonation of the HdmoPTA ligand, giving rise to the complex $[Ru(\eta^6\text{–}C_{10}H_{14})(Cl_2)(dmoPTA\text{-}\kappa P)]$ (**2**). The $^{31}P\{^1H\}$ NMR spectrum of **2** shows a singlet at −5.99 ppm in $CDCl_3$ (Figure S10), shifted approximately 3 ppm to downfield concerning

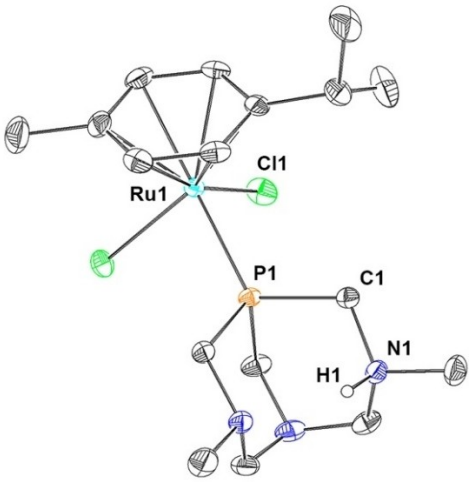


**Figure 2.** Crystal structure of **1** with ellipsoids at 25% probability. The triflate anion and all the hydrogen atoms except H1 are omitted for clarity.

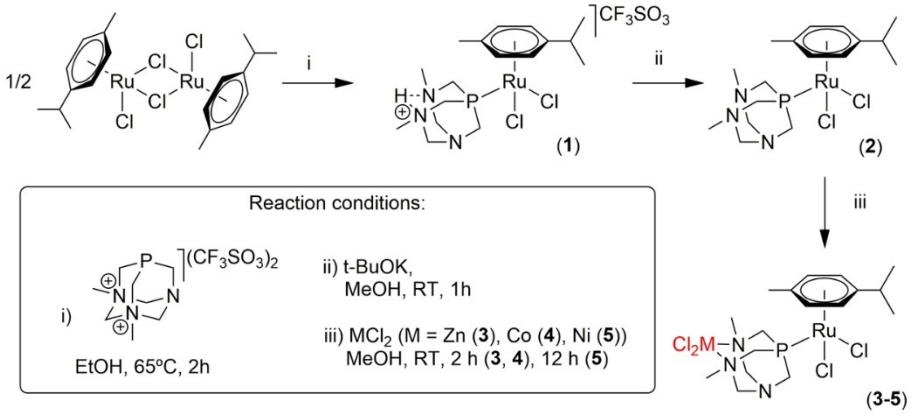


**Scheme 1.** Synthesis of **1**–**5**.

**1**, while its $^{1}$H NMR displays the protons of the dmoPTA at upfield and in a narrower range (2.30–3.84 ppm; Figure S8) than those for the HdmoPTA in **1** (2.58–4.42 ppm) and the signals of *p*-cymene do not suffer significant variations. In contrast, the differences in the signal chemical shifts in the $^{13}$C{$^{1}$H} NMR spectrum (Figure S9) are minimal between both complexes.

The bis-heterometallic complexes [Ru($\eta^6$–$C_{10}H_{14}$)($Cl_2$)-μ-dmoPTA-1κ*P*:2κ$^2$*N*,*N*′-$MCl_2$] (M=Zn (**3**), Co (**4**), Ni (**5**)) were synthesized by reacting the deprotonated complex **2** with the corresponding $MCl_2$ salt in dry MeOH (Scheme 1).

The NMR spectra of **3** in $CDCl_3$ shows many similarities with those of both **1** and **2**, such as a singlet at −6.43 ppm in the $^{31}$P{$^{1}$H} spectrum (Figure S18) shifted just 0.44 ppm at upfield to **2**, the $^{1}$H signals corresponding to the dmoPTA between 2.54 and 4.49 ppm, which is in a range closer to **1**, and the $^{1}$H resonances for the *p*-cymene. In contrast with **1** and **2** the $NCH_3$ protons are inequivalent and give rise to two singlets. The $^{13}$C{$^{1}$H} NMR spectrum of **3** (Figure S17) displays the expected signals and does not show any significant difference to those observed for complexes **1** and **2**. Complexes **4** and **5** were obtained from **2** by using a similar procedure to **3**, and therefore it is reasonable to suppose that they display a similar structure, changing only the metal chelated by the dmoPTA. The elemental analysis of **4** and **5** agrees with this assumption. The IR spectra of **3**–**5** are similar but quite different from the starting complex **1** (Figures S15, S23, and S27, respectively). In contrast to the diamagnetic complex **3**, the presence of $Co^{II}$ or $Ni^{II}$ in **4** and **5** respectively, precluded a full characterization by NMR as all the signals are particularly affected by the paramagnetism of the chelated metals, which supports that $Ni^{II}$ and $Co^{II}$ are effectively coordinated by the $CH_3N_{dmoPTA}$ atoms. The $^{31}$P{$^{1}$H} NMR spectra of both complexes in $CDCl_3$ also support this assumption as one broad unresolved signal arises at a very low field (**4**: 224.3 ppm; **5**: 132.16 ppm). This behavior was observed also for the similar complexes [RuClCp($PPh_3$)-μ-dmoPTA-1κ*P*:2κ$^2$*N*,*N*′-$MCl_2$][16b] (M=Co: 277 ppm; M=Ni: 81 ppm) and [RuCp($PPh_3$)$_2$-μ-dmoPTA-1κ*P*:2κ$^2$*N*,*N*′–$CoCl_2$] (211 ppm),[16d] in which chlorides are coordinated to the pendant metal, and is more pronounced than in complexes [RuClCp($PPh_3$)-μ-dmoPTA-1κ*P*:2κ$^2$*N*,*N*′-M(acac-κ$^2$*O*,*O*′)$_2$] (M=Co: 51.56 ppm; M=Ni: 62.6 ppm), where the coordination sphere of the metal is completed by acetylacetonate (acac) ligands.[16a] Also the $^{1}$H and $^{13}$C signals corresponding to the *p*-cymene are shifted significantly to the low field concerning the chemical shifts observed for this ligand in complex **3**.

## Crystal structure of 1, 3, and 5

Selected bond distances and angles for complex **1**, **3** and **5** are summarized in Table 1. Dark-red single crystals of **1** were obtained by evaporation from a methanolic solution. The asymmetric unit is constituted by one cationic complex [Ru($\eta^6$–$C_{10}H_{14}$)($Cl_2$)(HdmoPTA)]$^+$ and one disordered triflate. The unit cell contains four molecules of two different conformers (Figure 2). The coordination polyhedron around the Ru atom exhibits the expected distorted pseudo-octahedral geometry, similar to that of previously reported *p*-cymene–Ru complexes.[8] The *p*-cymene$_{cent}$–Ru1 bond length and *p*-cymene-Ru-$L_3$ angles are in agreement with reported values

**Table 1.** Selected bond lengths and angles for **1**, **3**, and **5**.

| | 1 | 3 | 5[a] |
|---|---|---|---|
| Length [Å] | | | |
| Ru1–Cl1 | 2.4079(11) | 2.4159(11) | 2.4250 |
| Ru1–Cl2 | 2.4104(11) | 2.4192(10) | 2.4054 |
| Ru1–P1 | 2.2970(11) | 2.2986(10) | 2.2934 |
| Ru1–*p*-cym$_{centr}$ | 1.707(10) | 1.708(10) | 1.7075 |
| N1–N2 | 2.713(1) | 2.951(5) | 2.9385 |
| M[b]–Cl3 | | 2.1967(11) | 2.206 |
| M[b]–Cl4 | | 2.2299(11) | 2.203 |
| M[b]–N1 | | 2.071(4) | 2.082 |
| M[b]–N2 | | 2.073(3) | 2.068 |
| Angle [°] | | | |
| Cl1–Ru1–Cl2 | 87.73(4) | 87.30(4) | 86.28 |
| P1–Ru1–Cl1 | 81.52(4) | 81.92(4) | 87.07 |
| P1–Ru1–Cl2 | 83.78(4) | 85.29(4) | 86.85 |
| P1–Ru1–*p*-cym$_{centr}$ | 132.1 | 130.63 | 127.81 |

[a] The mean values of the complex molecules found in the asymmetric unit are reported. [b] M=Zn (**3**), Ni (**5**).

(Ru1–$Cp_{cent}$ = 1.707(10) Å; mean Cp–$MCl_2$ angles: 84.34°).[18] The bond distances and angles in the HdmoPTA ligand are in agreement with those found in similar complexes.[19] It is important to point out that the hydrogen located between both $CH_3N_{dmoPTA}$ was localized during the structural refinement, being the distance between both nitrogen atoms of 2.713(1) Å, similar to that found in $[RuClCp(PPh_3)(HdmoPTA](CF_3SO_3)_3$ (N1–N3 = 2.702(6) Å).[14] The presence of this hydrogen leads to the alignment of the methyl groups (C6-N1-N2–C7 dihedral angle = 2.48(1)°).

Complexes **3** and **5** crystallized in the space group $P\bar{1}$ and $P2_1/n$, respectively. The asymmetric unit of **3** contains one molecule of $[Ru(\eta^6–C_{10}H_{14})(Cl_2)$-μ-dmoPTA-1κ*P*:2κ$^2$*N,N*′-$Zn(Cl)_2]$ that upon application of the symmetry rule generates the rotamer with the inverted *p*-cymene (Figure 3). For what concern to **5**, the asymmetric unit of its crystal structure contains two *p*-cymene rotamers of $[Ru(\eta^6–C_{10}H_{14})(Cl_2)$-μ-dmoPTA-1κ*P*:2κ$^2$*N,N*′-$Ni(Cl)_2]$ and one molecule of DMSO solvate (Figure 3). Bond distances and angles in these complexes are similar to those in complex **1**. In both cases, the metal chelated by the nitrogens of the dmoPTA, is coordinated in a tetrahedral fashion. The substitution of the proton in **1** for a $\{MCl_2\}$ moiety in **3** and **5** leads to a longer N1–N2 distance, which is slightly wider for **3**, where the bigger Zn is chelated (**3**: 2.951(5) Å, **5**: 2.9385 Å), and also to a better alignment between the methyl groups (C6-N1-N2-C7 dihedral angle = 0.92° (**3**), 1.94° (**Averaged, 5**)).

Although the M–Cl and M–N bond lengths in **3** and **5** are similar and comparable to what found for complex $[RuCp(PPh_3)_2$-μ-dmoPTA-1κ*P*:2κ$^2$*N,N*′-$ZnCl_2]CF_3SO_3$ and $[RuClCp(PPh_3)$-μ-dmoPTA-1κ*P*:2κ$^2$*N,N*′-$NiCl_2]$,[17] it should be noted that in **3** the Zn–Cl bonds are slightly less symmetric (Zn1–Cl3 = 2.1967(11) Å; Zn1–Cl4 = 2.2299(11)Å) and the Zn–N distances are significantly shorter than those found in complexes $[RuClCp(PPh_3)$-μ-dmoPTA-1κ*P*:2κ$^2$*N,N*′-$Zn(acac$-κ$^2$*O,O*′$)_2]$ (Zn1–N1 2.238(6) Å; Zn1–N2 2.278(7) Å).[16a] The dmoPTA in **3** and **5** is differently rotated about the Ru–P bond, so that in **3** the $\{ZnCl_2\}$ unit is pointing towards the *p*-cymene, while in **5** the $\{NiCl_2\}$ is directed downwards (Ru1-P1–C3-N3 dihedral angle = 178.3(2)° (**3**), −176.04° (**5**)). Finally, the crystal packing of **3** and **5** show only weak intermolecular interactions among the molecules.

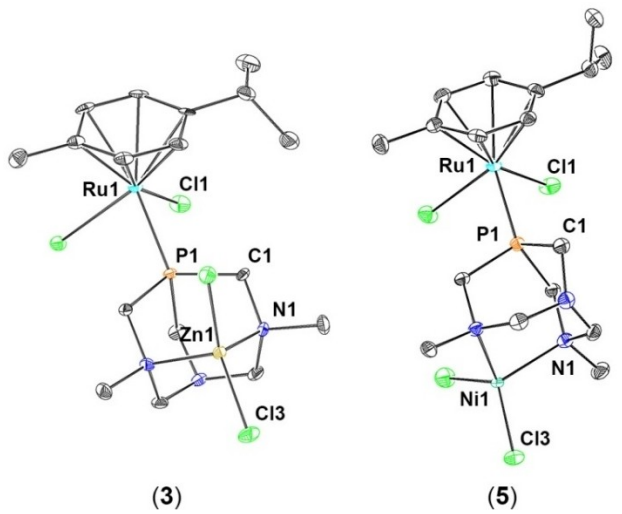


**Figure 3.** Crystal structure of **3** and **5** with ellipsoids at 50% probability. Hydrogen atoms and solvent molecules were omitted for clarity.

## Stability of the complexes in solution

The evaluation of the antiproliferative activity of the complexes requires their dissolution in a cellular culture medium that is mainly constituted by water. In some sample preparation protocols, mainly when the complex is not enough water soluble, it is previously dissolved in DMSO. It is important to determine if these complexes are the real active antiproliferative species or some products derived from their decomposition in media are active parts.

Therefore, the stability of the synthesized complexes in water and DMSO along the time, at room temperature and 37 °C was monitored by $^{31}P\{^1H\}$ NMR. Also, the stability of complexes in the mixture of DMSO/water (1:20) in the same condition of biological assay, was investigated (see the Supporting Information) and the results were the same with the spectra related to stability of complexes in water. Because, in the antiproliferative study in this work, the media contain a small percentage of DMSO, that is very low and negligible.

Complex **1** is soluble in both water and DMSO at room temperature. In the water, a major peak at −10.23 ppm (82%) is observed along with a side signal at −9.09 ppm (18%), which disappears upon the addition of 4 equivalents of NaCl. This fact suggests that the minor species is produced by substituted a molecule of water instead of one Cl. In any case, the $^{31}P\{^1H\}$ NMR of a water solution under the air of complex **1** does not change significantly during 49 h at room temperature and neither at 37 °C. Also, the solution containing 4 equivalents of NaCl is stable under the same condition. In contrast, solution of **1** in DMSO displays a $^{31}P\{^1H\}$ NMR constituted by a unique singlet at −9.09 ppm, which remains unchanged for 1 h at room temperature and only after 49 h small signals (< 3%) are observed at 7.50 and −6.89 ppm.

Similarly, the $^{31}P\{^1H\}$ NMR spectrum of **2** in water showed also two peaks: the main signal at −10.22 ppm (84%) and a minor at −9.52 ppm (16%), which also disappeared after adding 4 equivalents of NaCl into the solution. These two signals remained the most important after 2 h but some small peaks also appeared, that the most abundant located at −37.87 ppm (10%). Both the solution of **2** in water and presence of NaCl are stable under air at room temperature for 24 h, being the decomposition at 37 °C lesser than 15%. Complex **2** is stable in DMSO under air up to 4 h, then starts slowly to decompose but after 24 h the starting species is still the most abundant.

The $^{31}P\{^1H\}$ NMR spectrum of **3** in water is constituted by the main signal at −10.22 ppm (85%) and another at −9.17 ppm (15%), which are similar to those for **1** and remained the same after 24 h under air at room temperature

and 37 °C. As well as, the addition of 4 equiv of NaCl leads to disappearance of the minor signal. It is important to indicate that complex **3** is relatively stable also in DMSO at room temperature during 24 h as the $^{31}P\{^{1}H\}$ NMR shows the main signal at −8.77 ppm (> 95 %) and a broad signal at −4.02 ppm. After 15 h at 37 °C, these peaks disappear and new signals forms. The $^{31}P\{^{1}H\}$ NMR of complex **4** in water shows a unique sharp signal at −9.21 ppm, a similar chemical shift to that for complex **1**. This fact may suggest that the compound decomposes quickly when it is dissolved in water. Nevertheless, when water was removed and the resulting powder is dissolved in $CDCl_3$, the $^{31}P\{^{1}H\}$ NMR spectrum is identical to the spectra of previously **4** solution in $CDCl_3$. Therefore, the lack of broad band observed in organic solvents at the low field is not due to the decomposition of the compound. The stability of **4** in water versus time at room temperature and under air showed that after 1 h a small peak arises around 39 ppm, and after 24 h other signals are also observed. Nevertheless, the initial main singlet remains the most important. At 37 °C the observed behavior was similar; after 24 h decomposition was larger, but the starting complex remained as the most important species in the dissolution.

The dissolution of **4** in DMSO under air shows initially a unique broad signal at 138.05 ppm that remains the most abundant up to 30 minutes, then new peaks arise at 4.11 ppm, −2.99, −49.57, −70.57 and −88.29 ppm. This signal pattern remains practically unaltered for up to 4 days at room temperature. This process is faster at 37 °C. The dissolution of complex **5** in water initially shows a $^{31}P\{^{1}H\}$ NMR constituted by a broad signal at 45.17 ppm (> 95 %) and a singlet at −10.26 ppm, which slowly increases in intensity with time, becoming the most important after 24 h, but also new small singlets arise. At 37 °C the process was practically the same. Finally, the $^{31}P\{^{1}H\}$ NMR of complex **5** in DMSO shows a main broad signal (> 98 %) at 63.64 ppm at both room temperature and 37 °C and also small peaks at −4.04, −9.31, and −20.79 ppm are observed, which maintain the same proportion for 24 h.

To determine if some additional species not detectable by NMR generate in the solution, ESI-MS measurements were performed on freshly prepared solutions of the complexes in water and after 48 h. While in positive mode the fragmentation of the $\{MCl_2\}$ precluded the identification of the dimetallic complexes, only data recorded in negative mode were analyzed, showing the molecular peaks due to the corresponding complexes (Figures S42–S53). The results corroborate that after 48 h the starting complexes are still present in solution, supporting the data obtained by NMR spectroscopy.

## Antiproliferative activity and interaction with biosystems of the complexes

The synthesized complexes were evaluated against cancer cells and those with significant antiproliferative activity studied by specific experiments to determine their activity against normal cells and their possible action mechanisms. The antiproliferative activity of the complexes was evaluated towards human adenocarcinoma colon cancer cell line Caco-2/TC7 by using the MTT protocol at 72 h.[20] This cell line is useful for carrying out antiproliferative studies with cancer cells (5 days after seeding) but also with cells showing a spontaneous and homogeneous enterocytes differentiation,[21] which exhibit a well-differentiated brush border on the apical surface and tight junctions (14 days after seeding). In this monolayer form, cells resemble morphologically small intestine absorptive cells and therefore to study the cytotoxic and selectivity of our complexes on normal epithelial cells is feasible.[22] Different cultured cells were treated with increasing concentrations of the metallic derivatives (0–20 μM) and the obtained results (Table 2) showed that only bisheterometallic complexes **3**, **4** and **5** present antiproliferative effects toward tumor cells.

The cytotoxic activity of the three complexes against cancer cells is significantly better than that of cisplatin ($IC_{50} = 45.6 \pm 8.08$ μM)[23] and RAPTA–C, which are not cytotoxic on Caco-2 cell line.[24] The enhancement of the cytotoxic properties observed for bimetallic complexes are agree with other studies published on the literature, where a synergistic effect was shown.

Ruthenium(II)-*p*-cymene-phosphane derivative presents antimetastatic and potential cytotoxic properties,[25] therefore a combination of this moiety with a second fragment based on an active metal against cancer, may be useful to obtain novel chimeric chemotherapeutics with improved properties. This possible synergistic effect was observed in several gold(I)-ruthenium(II) complexes,[26] even with *p*-cymene ruthenium complexes.[27] The second metal was elected according to the great antiproliferative results of monometallic complexes based on zinc, cobalt, or nickel.[28] These complexes also induce interaction with DNA[29] (which is not observed for RAPTA derivatives)[30] and the activation of the caspase-mediated apoptotic pathway.

Generally, the enhancement of the cytotoxic effect is related to an improvement in their stability and solubility, besides this kind of bimetallic complexes are usually more selective towards cancer cells and less toxic to nontumorigenic human cell lines,[31] something that is coherent with our MTT results, where the cytotoxic effect was clearly enhanced. Additionally, it is remarkable to mention that neither of our complexes exhibited a cytotoxic effect on normal cells at the tested concentrations (Figure 4). Therefore, bimetallic complexes are great candidates to be considered as selective drugs against colon cancer cells.

The next step was to study the complex effects on the cell cycle and regulation of cell death. As known, one of the most significant aspects of different cancer cells from normal cells is

**Table 2.** Antiproliferative activity of synthesized complexes toward tumor Caco-2/TC7 cell line in vitro.

| Complex | 1 | 2 | 3 | 4 | 5 |
|---|---|---|---|---|---|
| $IC_{50}$ [μM] | ⩾ 20 | ⩾ 20 | 9.07 ± 0.27 | 5.40 ± 0.19 | 7.15 ± 0.30 |

[a] The results are expressed as mean values ± log SEM ($n \geq 12$ experiments).

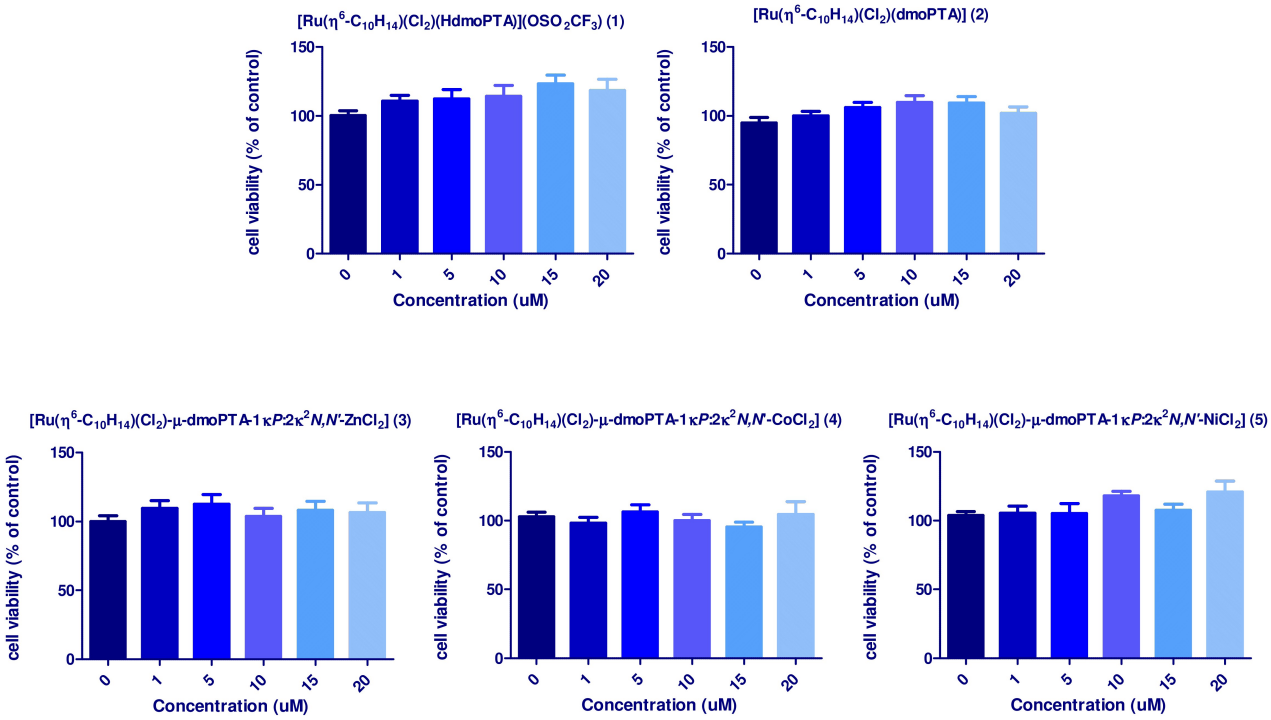


**Figure 4.** Cell viability of normal Caco-2 cells (15 days after seeding) treated with complexes **1**–**5** for 72 h. All the results are expressed as mean ± log SEM ($n \geq 12$ experiments).

their vertiginous speed of proliferation. The cell cycle is the procedure used by cells to grow and duplicate, consisting of single phases that are carefully controlled to detect any deviation of the process. The cell cycle is primarily regulated at the G1/S and G2/M phase transitions by a series of "checkpoints", which allow detecting any aberration in the cell during the process. Different possible evolution pathways can be chosen by the cell depending on how evolves such as cytokinesis, differentiation, quiescence and cell death.[32] Thus, a loss of proper checkpoint control in cancer cells contributes to tumorigenesis.[33] One of the challenges for antiproliferative therapy is, therefore, to achieve effective modulators of these checkpoints to arrest the cycle and induce cell death in those mutant cells such as tumor cells.[34] The effect of the complexes on the cell cycle of Caco-2 cells was studied by flow cytometry and is summarized in Table 3. The data show that the percentage of cells in G2/M phase is significantly higher for cells incubated with complex **4** than for control cells, suggesting that complex **4** may induce cell growth inhibition by arresting the cell cycle in G2/M phase. In contrast, complex **3** displayed a depletion of G0/G1 cell population that can be due to a slightly S-phase elongation. Finally, complex **5** did not seem to alter the normal cell cycle development. These observed differences show that the metal coordinates to the dmoPTA–$CH_3N$ atoms not only produce the antiproliferative activity of the complexes but, maybe more interesting, induce a differentiate activity on the cancer cells. It is also important to stress that complex **4**, the complex containing cobalt, performs the same arrest as oxaliplatin, the only platinum compound to show activity in colorectal cancer.[35]

**Table 3.** Cell populations in the different phases of the cell cycle.

| Complex | Cell population [%] G0/G1 | S | G2/M |
|---|---|---|---|
| control | 74.42 ± 2.42 | 18.22 ± 1.89 | 7.36 ± 0.98 |
| **3** | 71.99 ± 2.90* | 20.34 ± 4.60 | 7.60 ± 2.14 |
| **4** | 73.90 ± 2.08 | 18.51 ± 2.84 | 8.49 ± 1.56* |
| **5** | 74.94 ± 0.78 | 17.20 ± 0.30 | 7.86 ± 0.56 |

[a] All the results are expressed as mean ± log SEM ($n \geq 6$ experiments). * $P < 0.05$ with respect to the control.

Like some of our complexes, cisplatin also induces cell cycle arrest by its interaction with the DNA of cells. Regarding that our bimetallic complexes also present a square-planar environment of the second, we decided to investigate the possible interaction with DNA as cisplatin does. The interaction of the complexes **3**–**5** with calf thymus CT-DNA in Tris buffer was studied by UV-vis absorption titration. As an example, the absorption spectra of complex **3** in the absence and presence of increasing amounts of CT-DNA are given in Figure 5 (see the Supporting Information for all spectra). The addition of increasing amounts of CT-DNA caused hyperchromism in the main absorption bands of all three complexes, that suggest a moderate binding of **3**–**5** to CT-DNA.[36] Hyperchromism has been observed for the interaction of many drugs with DNA, ascribed to external contact (electrostatic binding),[37] or to the partial uncoiling of the helix structure of DNA, exposing more bases of the DNA.[38] Besides, a slight blue shift (3nm) was

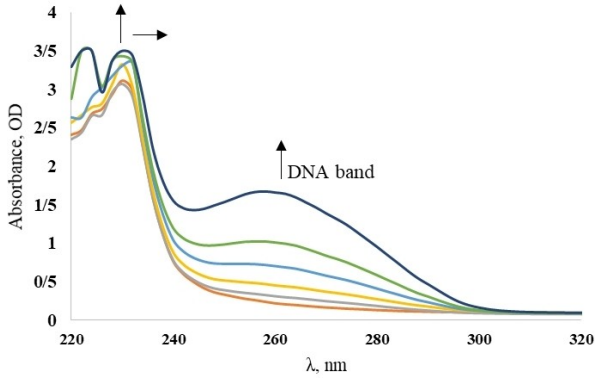


**Figure 5.** Absorption spectra of compound **3** (10 μM) in Tris buffer in the presence of increasing amounts of CT-DNA. The arrows indicate the absorbance changes upon increasing DNA concentration.

observed, something previously reported for Zn complexes.[39] All of these piece of evidence are consistent with an intercalative binding mode of our bimetallic complexes to CT-DNA.[40] The emerging band at 260 nm is due to CT-DNA, which increased as the concentration does.

With these results in mind, studies on how bimetallic complexes **3**–**5** participate in the externalization of phosphatidylserine (PS) and activation of the caspase cascade were performed,[41] which are two of the mechanisms involved in the apoptosis process. One of the most recognized differences between apoptotic and their neighbors' normal cells is the exposure of PS to the outer of the membrane in apoptotic cells, in contrast, to be located in the inner side of the normal cells. The combined action of annexin-V, which selectively binds to PS, and 7-AAD, which penetrates through the damaged membranes of both the late apoptotic and dead cells, allows distinguishing by flow cytometry between early and late apoptotic and dead cells. These experiments were carried out with undifferentiated Caco-2 cancer cells after incubation with complexes **3**–**5** (20 μM) for 24 h, while control cells were only treated with DMSO, the solvent used as a vehicle. As it is shown in Figure 6A, no significant increase in the apoptotic cell population was found after incubation with the complexes, indicating that their action mechanism is not through apoptosis induction by externalization of PS.

Generally, there are two major pathways for apoptosis: the intrinsic and extrinsic pathways. Both of these mechanism pathways involve the activation of a family of cysteine proteases that are named caspases.[42] There are two types of caspases, the executors that stay quiet until the other variety of caspase, the initiators, start the mechanism. Intrinsic and extrinsic pathways start by different initiators but both share the executors, caspase-3, −6 and −7.[43] The activity of the main executor caspases, caspase-3 and −7,[44] was determined by luminescence assays (Figure 6B), which showed that the three bimetallic complexes activate the activity of these caspases and, therefore, the three compounds induce programmed cell death by the caspase cascade.

Additionally, the capacity of complexes to produce oxidative stress damage in the cells was also evaluated as an inductor of death by disruption of the cellular redox homeostasis. In the cell, the balance between the oxidant and antioxidant species is carefully controlled to prevent oxidative damage of the main biomolecules such as proteins, lipids and DNA.[45] When this balance is corrupted and the molecules are damaged, the cell death process starts. Some anticancer agents act by inducing reactive oxygen and nitrogen species that usually are the initializing species for these processes.[46] The cell membrane is rich in polyunsaturated lipids and quite susceptible to be peroxidated if a rise of the oxidative species is provoked. Then, the two main species malondialdehyde (MDA) and hydroxyalkenals (4-HDA) are formed, which can be measured by Gerard–Monnier method.[47] In addition, proteins can suffer the oxidation and consequently generate carbonyl and thiol groups (–SH), which can easily derive to a dinitrophenyl hydrazone product by reaction with dinitrophenylhydrazine (DNPH) and the generated species detected by spectrophotometry.[48]

Figure 7 shows how the treatment of cells with complexes **3**–**5** did not afford higher MDA and 4-HDA content than control cells, so it can be assumed that our complexes do not induce peroxidation reactions in membrane lipids. Besides, no oxidized proteins were found as showed by the fact that the presence of carbonyl species in control and treated cells were not significantly different.

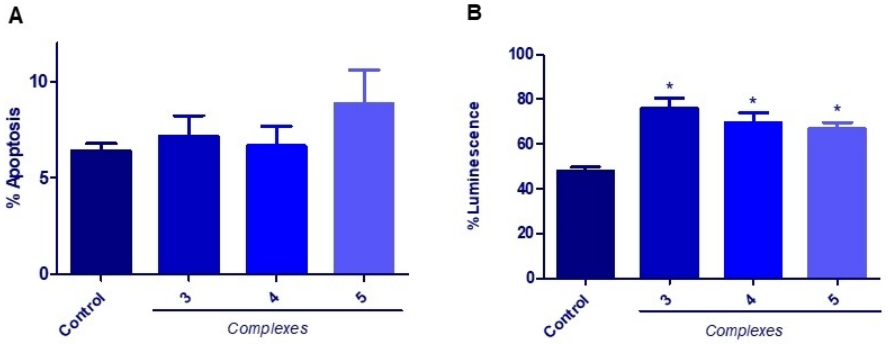


**Figure 6.** A) Early and late apoptosis values of cells treated with complexes **3**–**5** (20 μM, 24 h). B) Caspase activity values (background subtracted) with respect to the control. The results are expressed as mean values ± SEM ($n \geq 4$ experiments) * $P < 0.05$ respect to control.

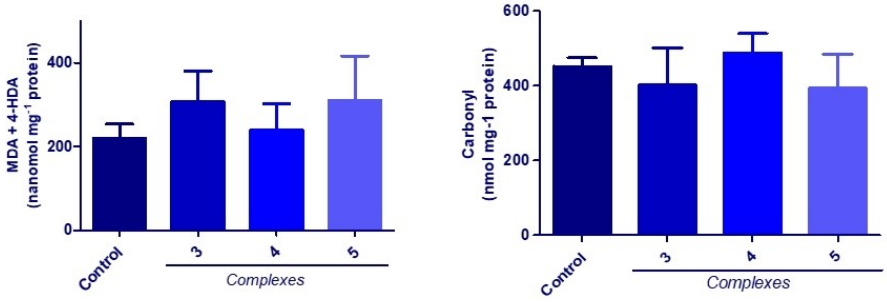


**Figure 7.** MDA + 4-HDA (left) and carbonyl (right) levels in Caco-2/TC7 cells treated with the vehicle DMSO (control) or the bimetallic complexes **3**–**5** (24 h, 20 μM). Values are expressed as mean values ± SEM ($n \geq 6$ experiments).

Therefore, oxidative stress did not seem to be the mechanism of action of our complexes and real-time-PCR (RT-PCR) studies were needed to determine whether the apoptotic mechanism can be induced by the regulation of pro- and anti-apoptotic genes by our complexes. It was evaluated the expression of important genes in the tumorigenesis process such as BIRC5, p53, Bax, PUMA, MDM2, APC, Bcl-2 and PARP-1 and codifying genes of caspase-3, caspase-8, caspase-9, and Trx.

Colorectal cancer (CRC) results as a consequence of a sequence of some genetic events to carcinoma from normal colonic cells. The genetic alterations that occurred in a single cell can be expanded to others if some important tumor-suppressor genes are silent. The best known tumor-suppressor genes in the CRC process are adenomatous polyposis coli (*APC*), DCC netrin 1 receptor (*DCC*), and *p53*. The *APC* gene is found to be inactive in most the CRC cases.[49] In fact, it is demonstrated that *APC* mutations promote the development of early adenomas and trigger other mutations in *KRAS*, *TP53* and *DCC* genes.[50] According to our results, only complex **5** increased the expression of *APC* gene (Figure 8), something very promising as this gene is involved in the earliest genetic events during the tumorigenesis process. By overexpressing this gene we may slow down the development of the tumor. Because the *APC* gene can influence on the protein TP53 that codifies the *p53* gene, the expression of *p53* was also studied. This also appears to be determinant in many CRC cases since it is inhibited in 70% of colorectal cancers.[51] It plays an important role in the cell cycle, apoptosis, and cellular growth because when damaged DNA is found in a cell, this cell is arrested in the G1 phase and prevents it from being replicated.[52] Moreover, other authors have also reported that *p53* can arrest the cell cycle at the G2/M phase.[53] In the performed cell-cycle studies in Caco-2 cells, we saw that complex **3** and **4** arrested cell cycle progress so, although it was expected these two complexes would up-regulate *p53*, we observed that the expression of *p53* was down-regulated after the incubation with these complexes. Complex **5** did not modify the *p53* expression, despite its influence on *APC* gene described above.

Both Bcl-2 and Bax are transcriptional targets for the tumor suppressor protein, p53.[54] The *p53* gene regulates in very different ways the activity of the Bcl-2 family proteins.[55] The antiapoptotic Bcl-2 protein inhibits cytochrome *c* release from the mitochondria and consequently, it blocks the caspase-mediated apoptosis.[56] Thus, the overexpression of the Bcl-2 is involved in the initiation of some tumors by decreasing apoptosis cell death.[57] In fact, some studies are reporting an overexpression of Bcl-2 in some patients with colorectal carcinomas.[57] The obtained results show that complexes **3**, **4** and **5** decrease the expression of Bcl-2, indicating that Bcl-2 might be a target for these complexes to inhibit the proliferation of colon cancer cells. In the case of complexes **3** and **4**, there is a downregulation of *p53* and Bcl-2. Patients with *p53*-negative status and downregulation of Bcl-2 present a better prognosis of life than those with positive Bcl-2 status.[58] It is believed that Bcl-2 status itself affects prognosis, something that may be explained by the fact that Bcl-2 inhibits apoptosis by controlling or even arresting cell cycle and thus, slowing down tumor cell growth avoiding reaching adenocarcinoma and staying as adenoma.[59] In our study, complexes **3** and **4** induced a down-regulation of p53, Bax, PUMA and MDM2. Direct activation of Bax by p53 mediates mitochondrial membrane permeabilization and apoptosis.[60] PUMA is a critical mediator of p53-dependent and -independent apoptosis induced by a wide variety of stimuli. PUMA directly binds and antagonizes all known antiapoptotic Bcl-2 family members to induce mitochondrial dysfunction and caspase activation.[61] The *p53* is negatively regulated by interaction with the oncoprotein MDM2. In this way, high levels of MDM2 lead to downregulation of tumor suppressive p53 pathways and the inhibition of MDM2–p53 interaction presents an appealing therapeutic strategy for the treatment of cancer.[62]

As has been mentioned, p53 and Bcl-2 are closely related to the caspase family activity. Caspase-3 study was conducted because both intrinsic and extrinsic cell death pathways converge on the activation of caspase-3,[63] but we also studied the expression of the initiators caspase-8 and −9 that act by different mechanisms.[64] The obtained results (Figure 8) indicate that complex **4** induces a down-regulation of caspases, −3, −8 and −9, while complex **3** decreases only the caspase-8 expression. In contrast, complex **5** did not modify the caspases expression. These results indicate that complex **5** would be the most efficient to activate the caspase pathway, as it does not modify the levels of caspases and activate them to induce apoptosis.

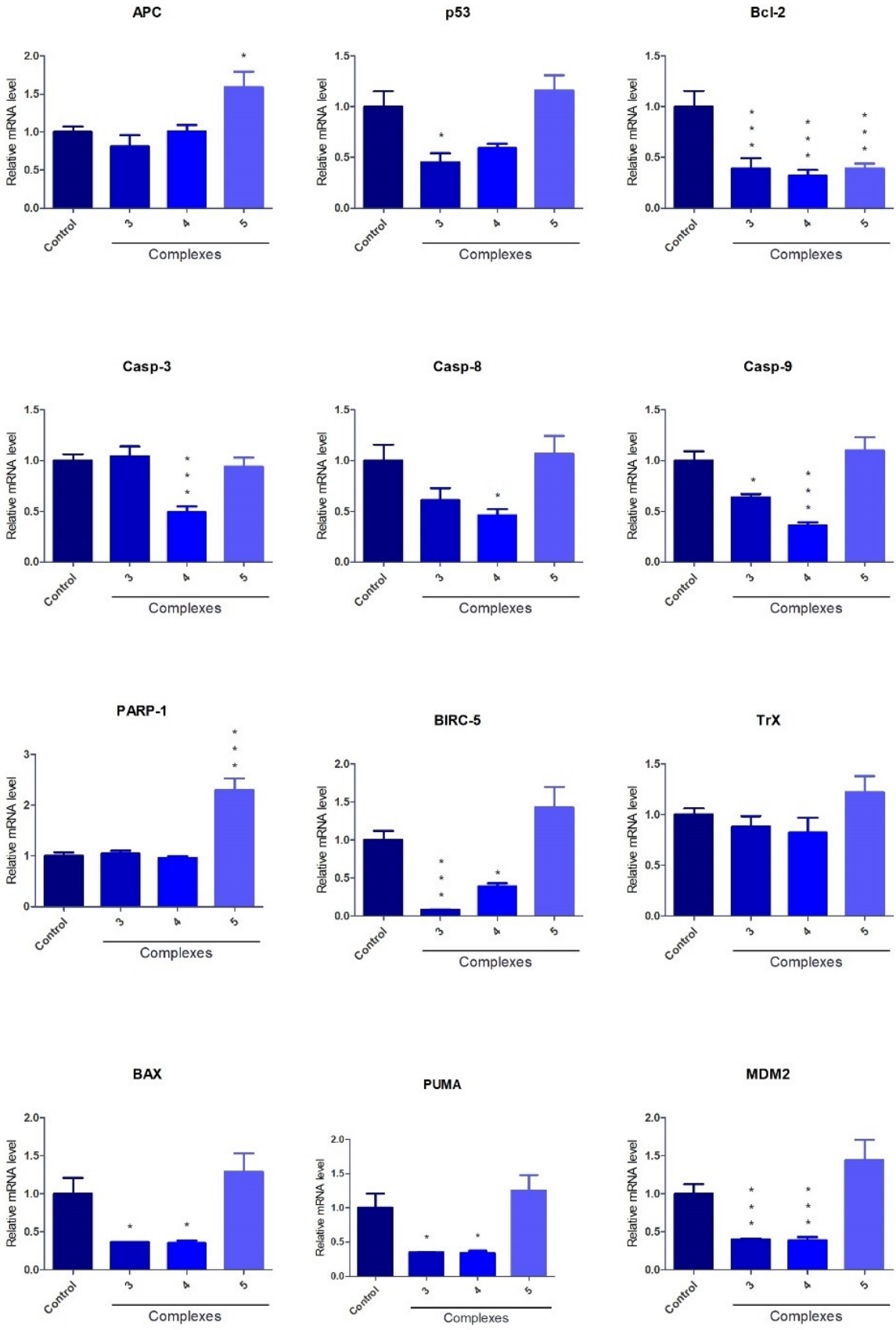


**Figure 8.** Expression of apoptotic and anti-apoptotic genes induced by complexes **3**–**5** in Caco-2/TC7 cells, determined by RT-PCR. Values are expressed as mean values ± SEM ($n \geq 6$ experiments). * $P < 0.05$, ** $P < 0.01$, *** $P < 0.005$

The caspase family, among other processes, eliminates poly-ADP-ribose-polymerase (PARP), which plays a crucial role in DNA repair.[65] Its fundamental role is the protection of the genome stability and also participates in many different ways of DNA repair.

Cancer cells often have defects in repair pathways that make them more susceptible to DNA damage, such as the mentioned inhibition of p53 gene. For this reason, over-expression of PARP-1 is found in several primary malignancies, although cancers such as adrenal, bone, colon and prostate carcinoma tissues do not show significant overexpression of PARP-1.[66] The role of PARP-1 in tumor development is still unclear, according to our results, complex **5** increases the expression of PARP-1 comparing to control cells, something that may promote the genome stability and avoid the accumulation of mutations.

In addition, caspases and p53 influence the expression of other genes such as BIRC5.[67] BIRC5 (also known as Survivin) is essential for cell division and can inhibit cell death, that is why it is usually found to be overexpressed in some cancer.[68] Besides, BIRC5 has frequently been associated with resistance of cancer cells to chemo- or radiotherapy.[69] Our studies showed that complexes **3** and **4** downregulated the expression of BIRC5 gene, indicating that these complexes might be useful in the chemotherapy field.

Finally, we evaluated the activity of the thioredoxin family (Trx) as it plays an important role in redox control, protecting cells from the damage of free radicals.[70] The antioxidant defense is especially important in terms of cancer therapy,[71] since the higher metabolism of tumor cells implies more concentration of ROS species and the overexpression of antioxidant proteins.[71] Noticeably, none of our complexes present any effect on Trx expression.

The biological results clearly show how the participation of a second metal is very important to induce a significant antiproliferative activity, which is better than that for cisplatin and RAPTA–C, in ruthenium complexes containing *p*-cymene and dmoPTA. Nevertheless, and probably more important, the bimetallic complexes do not display toxicity against normal cells, but also their action mechanism is different depending on the nature of the second metal. It is important to point out that neither Co, Ni nor Zn is known to be an antiproliferative active metal, but as in the case of the family of complexes [RuClCp($PPh_3$)-μ-dmoPTA-1κ*P*:2κ$^2$*N*,*N*′-$MCl_2$], [RuCp($PPh_3$)$_2$-μ-dmoPTA-1κ*P*:2κ$^2$*N*,*N*′-$MCl_2$]($CF_3SO_3$) and [RuClCp($PPh_3$)-μ-dmoPTA-1κ*P*:2κ$^2$*N*,*N*′-M(acac-κ$^2$*O*,*O*′)$_2$],[19] their participation in the complex composition lead to increase notably the antiproliferative activity of the complexes. Stability experiments showed that bimetallic complexes are stable enough in water and DMSO for considering them as the active species penetrating the cells. Therefore, the linkage of a Ru atom with a heterometal by the ligand dmoPTA gives rise to a bis-heterometallic system that activates the apoptosis cell processes by different action mechanisms depending on the metal bonded to the $CH_3N_{dmoPTA}$ atoms.

## Conclusions

The RAPTA type complex [Ru-(η$^6$–$C_{10}H_{14}$)($Cl_2$)(HdmoPTA)]($OSO_2CF_3$) (**1**) has been synthesized and deprotonated to afford the complex [Ru-(η$^6$–$C_{10}H_{14}$)($Cl_2$)(dmoPTA)] (**2**), which was further treated with $ZnCl_2$, $CoCl_2$, and $NiCl_2$ to give the bimetallic complexes [Ru(η$^6$–$C_{10}H_{14}$)($Cl_2$)-μ-dmoPTA-1κ*P*:2κ$^2$*N*,*N*′-$MCl_2$], in which a {$ZnCl_2$} (**3**), {$CoCl_2$} (**4**) or a {$NiCl_2$} (**5**) is chelated by the $NCH_3$ atoms of the dmoPTA. The antiproliferative activity of the complexes was evaluated against colon cancer cell line Caco-2/TC7 by using the MTT protocol. The monometallic ruthenium complexes **1** and **2** were found to be inactive against these cancer cells, but the bimetallic complexes **3**–**5** display a significantly better activity ($IC_{50}$ **3**: 9.07 ± 0.27; $IC_{50}$ **4**: 5.40 ± 0.19; $IC_{50}$ **5**: 7.15 ± 0.30) than cisplatin ($IC_{50}$ = 45.6 ± 8.08 μM) and RAPTA–C. Notably, despite their large antiproliferative activity, all the three complexes are nontoxic against normal cells. Stability experiments showed that bimetallic complexes are stable enough in water and DMSO to be considered as active species. It is necessary to remember that neither Co, Ni nor Zn is known to be an antiproliferative metal, but their presence in compounds **3**–**5** notably increases the cytotoxicity, and, depending on the metal, a different mechanism of action is induced. Flow cytometry studies showed that complex **4** can inhibit cell growth by stopping the G2/M phase of the cell cycle, whereas **3** causes depletion of G0/G1 cell population, and **5** does not alter the normal cell cycle. However, all of them seem to interact with DNA. Apoptosis studies showed that complexes **3**, **4** and **5** do not induce a significant increase in apoptotic cell population, and therefore this process was not promoted by the externalization of phosphatidylserine (PS). Nevertheless, it was also found that the three complexes activate caspases-3 and −7, inducing programmed cell death by the caspase cascade. The three complexes do not cause the formation of higher malondialdehyde and hydroxyalkenals, and for this reason, we can suppose that they do not induce peroxidation in membrane lipids, and therefore no oxidized proteins were produced when used. Complexes **3**–**5** can regulate the expression of genes involved in colon cancer development. Complexes **3** and **4** downregulate *Bcl-2*, a gene that inhibits apoptosis by controlling the cell cycle, and *BIRC-5*, a gene that inhibits cell death. Complex **5** inhibits *Bcl-2* expression and upregulates *PARP-1*, a gene involved in genome stability, and *APC*, a tumor-suppressor gene.

The proved ability of this class of complexes to activate different apoptotic mechanisms depending on the nature of the second metal coordinated to the dmoPTA ligand opens the door to evaluate other possible combinations, considering also metals that are currently not known to be antiproliferative. Finally, experiments to understand how the bimetallic complexes work inside the cell are in progress, as well as the synthesis of new bis-heterometallic and multi-heterometallic complexes.

Deposition Numbers 2085510 (**1**), 2085511 (**3**) and 2085513 (**5**) contain the supplementary crystallographic data for this paper. These data are provided free of charge by the joint

Cambridge Crystallographic Data Centre and Fachinformationszentrum Karlsruhe Access Structures service.

## Acknowledgements

The authors thank the University of Almeria for the project PPUENTE2020/011 and the Junta de Andalucía for funding research PAI team FQM-317 and Excellence Project PY20 00791. Tanks are also given the European Commission FEDER program for co-financing the projects. Besides, this work partially funded by Gobierno de Aragón (Spain) (Grupo Reconocido A02 17R) and associated EU Regional Developments Funds. N.K. thanks the Erasmus + Ka1 Mobility for a stay grant at the University of Almeria. We are very grateful to Dr. José Emilio Mesonero (Departamento de Farmacología, Fisiología y Medicina Legal y Forense, Universidad de Zaragoza, Spain) for providing the Caco-2/TC7 cell line. The authors thank the Centro de Investigación Biomédica de Aragón (CIBA) for technical assistance.

## Conflict of Interest

The authors declare no conflict of interests.

**Keywords:** antiproliferative activity · apoptosis · bis-heterometallic complexes · caspases · cell cycle · ruthenium

[1] K. D. Mjos, C. Orvig, *Chem. Rev.* **2014**, *114*, 4540–4563.
[2] a) X. Wang, Z. Guo, *Chem. Soc. Rev.* **2013**, *42*, 202–224; b) N. Pabla, Z. Dong, *Kidney Int.* **2008**, *73*, 994–1007; c) S. A. Aldossary, *Biomed. Pharmacol. J.* **2019**, *12*, 7–15.
[3] a) M. Abid, F. Shamsi, A. Azam, *Mini-Rev. Med. Chem.* **2016**, *16*, 772–786; b) S. Y. Lee, C. Y. Kim, T.-G. Nam, *Drug Des. Dev. Ther.* **2020**, *14*, 5375.
[4] S. Betanzos-Lara, L. Salassa, A. Habtemariam, P. J. Sadler, *Chem. Commun.* **2009**, 6622–6624.
[5] a) Y. K. Yan, M. Melchart, A. Habtemariam, P. J. Sadler, *Chem. Commun.* **2005**, 4764–4776; b) H. Chen, J. A. Parkinson, S. Parsons, R. A. Coxall, R. O. Gould, P. J. Sadler, *J. Ame. Chem. Soc.* **2002**, *124*, 3064–3082; c) F. Wang, H. Chen, J. A. Parkinson, P. d. S. Murdoch, P. J. Sadler, *Inorg. Chem.* **2002**, *41*, 4509–4523; d) F. Wang, J. Bella, J. A. Parkinson, P. J. Sadler, *JBIC J. Biol. Inorg. Chem.* **2005**, *10*, 147–155.
[6] a) F. Frausin, V. Scarcia, M. Cocchietto, A. Furlani, B. Serli, E. Alessio, G. Sava, *J. Pharmacol. Exp. Ther.* **2005**, *313*, 227–233; b) B. Serli, E. Zangrando, T. Gianferrara, L. Yellowlees, E. Alessio, *Coord. Chem. Rev.* **2003**, *245*, 73–83; c) G. Sava, R. Gagliardi, *Anticancer Res.* **1999**, *19*, 969.
[7] C. Allardyce, P. Dyson, D. Ellis, S. Heath, *Chem. Commun.* **2001**, 1396–1397.
[8] B. S. Murray, M. V. Babak, C. G. Hartinger, P. J. Dyson, *Coord. Chem. Rev.* **2016**, *306*, 86–114.
[9] a) A. Guerriero, M. Peruzzini, L. Gonsalvi, *Coord. Chem. Rev.* **2018**, *355*, 328–361; b) J. Bravo, S. Bolaño, L. Gonsalvi, M. Peruzzini, *Coord. Chem. Rev.* **2010**, *254*, 555–607; c) A. D. Phillips, L. Gonsalvi, A. Romerosa, F. Vizza, M. Peruzzini, *Coord. Chem. Rev.* **2004**, *248*, 955–993.
[10] a) L. Biancalana, S. Fulignati, C. Antonetti, S. Zacchini, G. Provinciali, G. Pampaloni, A. M. R. Galletti, F. Marchetti, *New J. Chem.* **2018**, *42*, 17574–17586; b) J. Furrer, G. Süss-Fink, *Coord. Chem. Rev.* **2016**, *309*, 36–50; c) V. Studer, N. Anghel, O. Desiatkina, T. Felder, G. Boubaker, Y. Amdouni, J. Ramseier, M. Hungerbühler, C. Kempf, J. T. Heverhagen, *Pharmaceutica* **2020**, *13*, 471; d) P. Zhang, P. J. Sadler, *J. Organomet. Chem.* **2017**, *839*, 5–14; e) A. Bergamo, P. J. Dyson, G. Sava, *Coord. Chem. Rev.* **2018**, *360*, 17–33.
[11] A. Romerosa, T. Campos-Malpartida, C. Lidrissi, M. Saoud, M. Serrano-Ruiz, M. Peruzzini, J. A. Garrido-Cárdenas, F. García-Maroto, *Inorg. Chem.* **2006**, *45*, 1289–1298.
[12] a) L. Hajji, C. Saraiba-Bello, A. Romerosa, G. Segovia-Torrente, M. Serrano-Ruiz, P. Bergamini, A. Canella, *Inorg. Chem.* **2011**, *50*, 873–882; b) L. Hajji, C. Saraiba-Bello, G. Segovia-Torrente, F. Scalambra, A. Romerosa, *Eur. J. Inorg. Chem.* **2019**, 4078–4086.
[13] a) A. Romerosa, M. Saoud, T. Campos-Malpartida, C. Lidrissi, M. Serrano-Ruiz, M. Peruzzini, J. A. Garrido, F. García-Maroto, *Eur. J. Inorg. Chem.* **2007**, *2007*, 2803–2812; b) L. Hajji, C. Saraiba-Bello, F. Scalambra, G. Segovia-Torrente, A. Romerosa, *J. Inorg. Biochem.* **2021**, *218*, 111404.
[14] A. Mena-Cruz, P. Lorenzo-Luis, A. Romerosa, M. Saoud, M. Serrano-Ruiz, *Inorg. Chem.* **2007**, *46*, 6120–6128.
[15] A. Mena-Cruz, P. Lorenzo-Luis, A. Romerosa, M. Serrano-Ruiz, *Inorg. Chem.* **2008**, *47*, 2246–2248.
[16] a) A. Mena-Cruz, P. Lorenzo-Luis, V. Passarelli, A. Romerosa, M. Serrano-Ruiz, *Dalton. Trans.* **2011**, *40*, 3237–3244; b) M. Serrano-Ruiz, L. M. Aguilera-Sáez, P. Lorenzo-Luis, J. M. Padrón, A. Romerosa, *Dalton Trans.* **2013**, *42*, 11212–11219; c) Z. Mendoza, P. Lorenzo-Luis, M. Serrano-Ruiz, E. Martín-Batista, J. M. Padrón, F. Scalambra, A. Romerosa, *Inorg. Chem.* **2016**, *55*, 7820–7822; d) Z. Mendoza, P. Lorenzo-Luis, F. Scalambra, J. M. Padrón, A. Romerosa, *Dalton Trans.* **2017**, *46*, 8009–8012; e) F. Scalambra, N. Holzmann, L. Bernasconi, S. Imberti, A. Romerosa, *Eur. J. Inorg. Chem.* **2019**, 1162–1169.
[17] Z. Mendoza, P. Lorenzo-Luis, F. Scalambra, J. M. Padrón, A. Romerosa, *Eur. J. Inorg. Chem.* **2018**, 4684–4688.
[18] J. Mitchell, J. H. Robertson, P. R. Raithby, *Cambridge Structural Database* **2020**.
[19] F. Scalambra, P. Lorenzo-Luis, I. de los Ríos, A. Romerosa, *Eur. J. Inorg. Chem.* **2019**, *2019*, 1529–1538.
[20] T. Mosmann, *J. Immunol. Methods* **1983**, *65*, 55–63.
[21] a) V. Meunier, M. Bourrie, Y. Berger, G. Fabre, *Cell Biol. Toxicol.* **1995**, *11*, 187–194; b) M. Rousset, *Biochimie.* **1986**, *68*, 1035–1040.
[22] H.-P. Hauri, E. E. Sterchi, D. Bienz, J. Fransen, A. Marxer, *J. Cell Biol.* **1985**, *101*, 838–851.
[23] E. García-Moreno, A. Tomás, E. Atrián-Blasco, S. Gascón, E. Romanos, M. J. Rodriguez-Yoldi, E. Cerrada, M. Laguna, *Dalton Trans.* **2016**, *45*, 2462–2475.
[24] A. Mondal, P. Paira, *Dalton Trans.* **2020**, *49*, 12865–12878.
[25] P. Nowak-Sliwinska, *J. Med. Chem.* **2011**, *54*, 3895–3902.
[26] L. K. Batchelor, D. Ortiz, P. J. Dyson, *Inorg. Chem.* **2019**, *58*, 2501–2513.
[27] L. Massai, J. Fernández-Gallardo, A. Guerri, A. Arcangeli, S. Pillozzi, M. Contel, L. Messori, *Dalton Trans.* **2015**, *44*, 11067–11076.
[28] a) B. Şen, H. K. Kalhan, V. Demir, E. E. Güler, H. A. Kayalı, E. Subaşı, *Mat. Sci. Eng. C.* **2019**, *98*, 550–559; b) Z. Shokohi-Pour, H. Chiniforoshan, M. R. Sabzalian, S.-A. Esmaeili, A. A. Momtazi-Borojeni, *J. Biomol. Struct. Dyn.* **2018**, *36*, 532–549.
[29] F. Ramilo-Gomes, Y. Addis, I. Tekamo, I. Cavaco, D. L. Campos, F. R. Pavan, C. S. Gomes, V. Brito, A. O. Santos, F. Domingues, *J. Inorg. Biochem.* **2021**, *216*, 111331.
[30] A. R. Simović, R. Masnikosa, I. Bratsos, E. Alessio, *Coord. Chem. Rev.* **2019**, *398*, 113011.
[31] J. Fernández-Gallardo, B. T. Elie, M. Sanaú, M. Contel, *Chem. Commun.* **2016**, *52*, 3155–3158.
[32] H. S. Bell, K. M. Ryan, *Eur. J. Cancer.* **2005**, *41*, 206–215.
[33] A. G. Paulovich, D. P. Toczyski, L. H. Hartwell, *Cell.* **1997**, *88*, 315–321.
[34] K. R. Webster, *Chem. Res. Toxicol.* **2000**, *13*, 940–943.
[35] S. William-Faltaos, D. Rouillard, P. Lechat, G. Bastian, *Fund. Clin. Pharmacol.* **2007**, *21*, 165–172.
[36] S. Radisavljević, I. Bratsos, A. Scheurer, J. Korzekwa, R. Masnikosa, A. Tot, N. Gligorijević, S. Radulović, A. R. Simović, *Dalton Trans.* **2018**, *47*, 13696–13712.
[37] R. F. Pasternack, E. J. Gibbs, J. J. Villafranca, *Biochem.* **1983**, *22*, 5409–5417.
[38] G. Pratviel, J. Bernadou, B. Meunier, *Adv. Inorg. Chem.* **1998**, *45*, 251.
[39] N. Shahabadi, Z. Ghasemian, S. Hadidi, *Bioinorg. Chem. Appl.* **2012**, *2012*, 1-9.
[40] Y. Sun, S. Bi, D. Song, C. Qiao, D. Mu, H. Zhang, *Sens. Actuators B.* **2008**, *129*, 799–810.
[41] R. C. Taylor, S. P. Cullen, S. J. Martin, *Nat. Rev. Mol. Cell Biol.* **2008**, *9*, 231–241.
[42] S. Elmore, *Toxico. Pathol.* **2007**, *35*, 495–516.
[43] C.-Y. Chang, C.-Y. Chiang, Y.-W. Chiang, M.-W. Lee, C.-Y. Lee, H.-Y. Chen, H.-W. Lin, Y.-H. Kuan, *Polymer* **2020**, *12*, 1398.
[44] K. Nichani, J. Li, M. Suzuki, J. P. Houston, *Cytometry Part A* **2020**, *97*, 1265–1275.
[45] L. He, T. He, S. Farrar, L. Ji, T. Li, X. Ma, *Cell. Physiol. Biochem.* **2017**, *44*, 532–553.

[46] a) K.-B. Huang, F.-Y. Wang, X.-M. Tang, H.-W. Feng, Z.-F. Chen, Y.-C. Liu, Y.-N. Liu, H. Liang, *J. Med. Chem.* **2018**, *61*, 3478–3490; b) E. Abas, N. Espallargas, G. Burbello, J. E. Mesonero, A. Rodriguez-Dieguez, L. Grasa, M. Laguna, *Inorg. Chem.* **2019**, *58*, 15536–15551.
[47] D. Gérard-Monnier, I. Erdelmeier, K. Régnard, N. Moze-Henry, J.-C. Yadan, J. Chaudiere, *Chem. Res. Toxicol.* **1998**, *11*, 1176–1183.
[48] a) R. L. Levine, *Free Radical Biol. Med.* **2002**, *32*, 790–796; b) R. L. Levine, D. Garland, C. N. Oliver, A. Amici, I. Climent, A.-G. Lenz, B.-W. Ahn, S. Shaltiel, E. R. Stadtman, *Meth. Enzymol.* **1990**, *186*, 464–478.
[49] a) E. R. Fearon, *Annu. Rev. Pathol. Mech. Disease.* **2011**, *6*, 479–507; b) A. S. Aghabozorgi, A. Bahreyni, A. Soleimani, A. Bahrami, M. Khazaei, G. A. Ferns, A. Avan, S. M. Hassanian, *Biochimie* **2019**, *157*, 64–71.
[50] E. R. Fearon, B. Vogelstein, *Cell.* **1990**, *61*, 759–767.
[51] A. Watson, *Gut.* **2004**, *53*, 1701–1709.
[52] a) J. W. Harper, G. R. Adami, N. Wei, K. Keyomarsi, S. J. Elledge, *Cell.* **1993**, *75*, 805–816; b) W. S. El-Deiry, J. W. Harper, P. M. O′Connor, V. E. Velculescu, C. E. Canman, J. Jackman, J. A. Pietenpol, M. Burrell, D. E. Hill, Y. Wang, *Cancer Res.* **1994**, *54*, 1169–1174.
[53] J. Martín-Caballero, J. M. Flores, P. García-Palencia, M. Serrano, *Cancer. Res.* **2001**, *61*, 6234–6238.
[54] A. Basu, S. Haldar, *Mol. Hum. Reprod.* **1998**, *4*, 1099–1109.
[55] M. Hemann, S. Lowe, *Cell Death Differ.* **2006**, *13*, 1256.
[56] C. A. Elena-Real, A. Díaz-Quintana, K. González-Arzola, A. Velázquez-Campoy, M. Orzáez, A. López-Rivas, S. Gil-Caballero, Á. Miguel, I. Díaz-Moreno, *Cell. Death. Disease.* **2018**, *9*, 1–12.
[57] P. Ramesh, J. P. Medema, *Apoptosis.* **2020**, *25*, 305–320.
[58] L. Kaklamanis, A. Savage, N. Mortensen, P. Tsiotos, I. Doussis-Anagnostopoulou, S. Biddolph, R. Whitehouse, A. L. Hrris, K. C. Gatter, *J. Pathol.* **1996**, *179*, 10–14.
[59] N. Bonnefoy-Berard, A. Aouacheria, C. Verschelde, L. Quemeneur, A. Marçais, J. Marvel, *Biochimica. Sci.* **2004**, *303*, 1010–1014.
[60] J. Yu, L. Zhang, *Oncogene.* **2008**, *27*, S71-S83.
[61] U. M. Moll, O. Petrenko, *Mol. Cancer Res.* **2003**, *1*, 1001–1008.
[62] C. Pisani, M. Ramella, R. Boldorini, G. Loi, M. Billia, F. Boccafoschi, A. Volpe, M. Krengli, *Sci. Rep.* **2020**, *10*, 1–10.
[63] J. Li, J. Yuan, *Oncogene.* **2008**, *27*, 6194–6206.
[64] M. Los, M. Mozoluk, D. Ferrari, A. Stepczynska, C. Stroh, A. Renz, Z. Herceg, Z.-Q. Wang, K. Schulze-Osthoff, *Mol. Biol. Cell.* **2002**, *13*, 978–988.
[65] V. Ossovskaya, I. C. Koo, E. P. Kaldjian, C. Alvares, B. M. Sherman, *Genes. Cancer.* **2010**, *1*, 812–821.
[66] S. Zhao, J. Cai, H. Bian, L. Gui, F. Zhao, *Cancer Invest.* **2009**, *27*, 636–640.
[67] S. P. Wheatley, D. C. Altieri, *J. Cell Sci.* **2019**, *132*, 1-8.
[68] J. Lu, M. Tan, W.-C. Huang, P. Li, H. Guo, L.-M. Tseng, X.-h. Su, W.-T. Yang, W. Treekitkarnmongkol, M. Andreeff, *Clin. Cancer. Res.* **2009**, *15*, 1326–1334.
[69] F. Mohammadi, A. Soltani, A. Ghahremanloo, H. Javid, S. I. Hashemy, *Cancer Chemother. Pharmacol.* **2019**, *84*, 925–935.
[70] V. Sosa, T. Moliné, R. Somoza, R. Paciucci, H. Kondoh, M. E. LLeonart, *Age. Res. Rev.* **2013**, *12*, 376–390.
[71] T. C. Karlenius, K. F. Tonissen, *Cancers.* **2010**, *2*, 209–232.

Manuscript received: August 20, 2021
Accepted manuscript online: November 21, 2021
Version of record online: December 8, 2021